5.3 TWO HARMONIC FORCES: FREE-FREE BEAM

The previous applications were limited to the estimation of a single harmonic force. In this section the free-free beam was invoked once again to investigate the extension of the force identification methods in the frequency domain to determine two harmonic forces acting on the beam.

5.3.1 Details of the Experimental Set-up

The components of the measurement system are essentially the same as before, but have been extended to cater for two exciters and are shown in Figure 5.14.

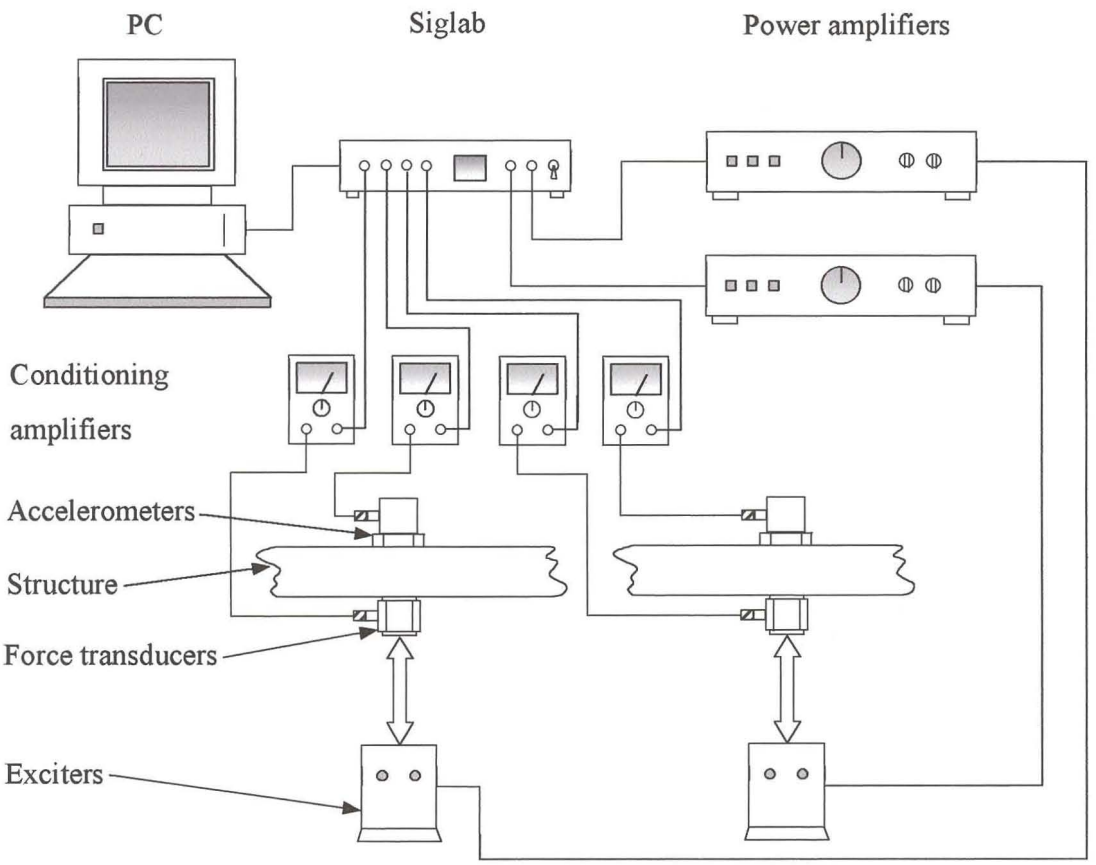

Figure 5.14 – Measurement system used for the identification of two harmonic forces

5.3.2 The Measurements

Eleven acceleration signals were recorded with two roving accelerometers. The two harmonic forces, with frequency content 380 Hz and 250 Hz, were applied to the free-free aluminium beam at two different positions (position 5 and 8 respectively), the inertance frequency response functions having already been determined with the MIMO excitation (refer to Section 2.4). As mentioned before, this was done to

account for the distortion of the natural frequencies of the beam due to the attachment of the two exciters. It can be seen from Figures 5.15 and 5.16 that the first five bending modes spanned the chosen frequency range from 0 Hz to 500 Hz.

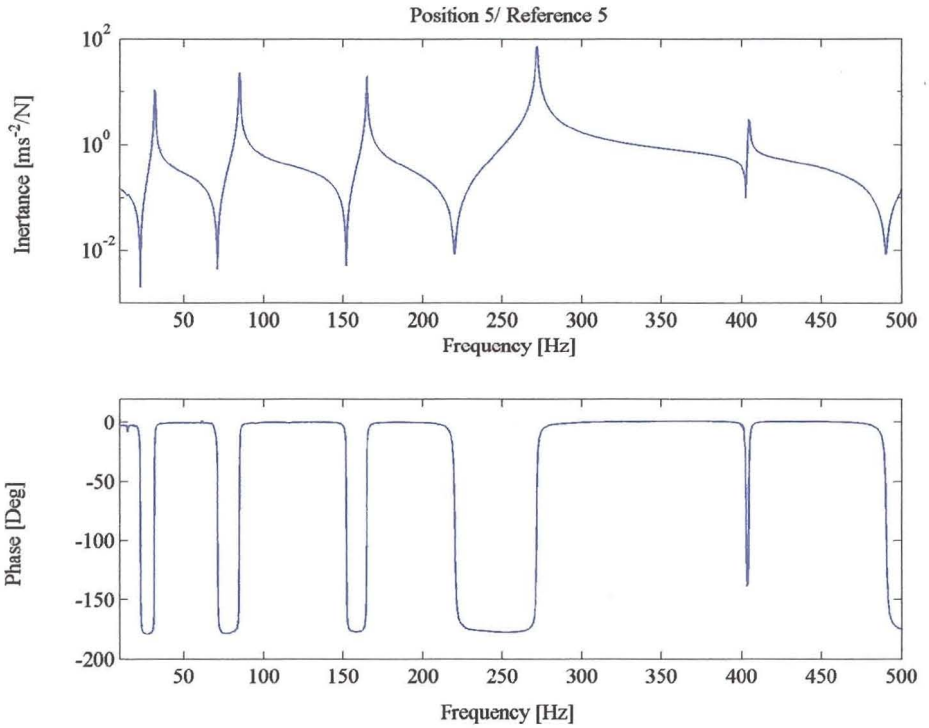

Figure 5.15 – Measured point inertance for the free-free beam corresponding to reference position 5

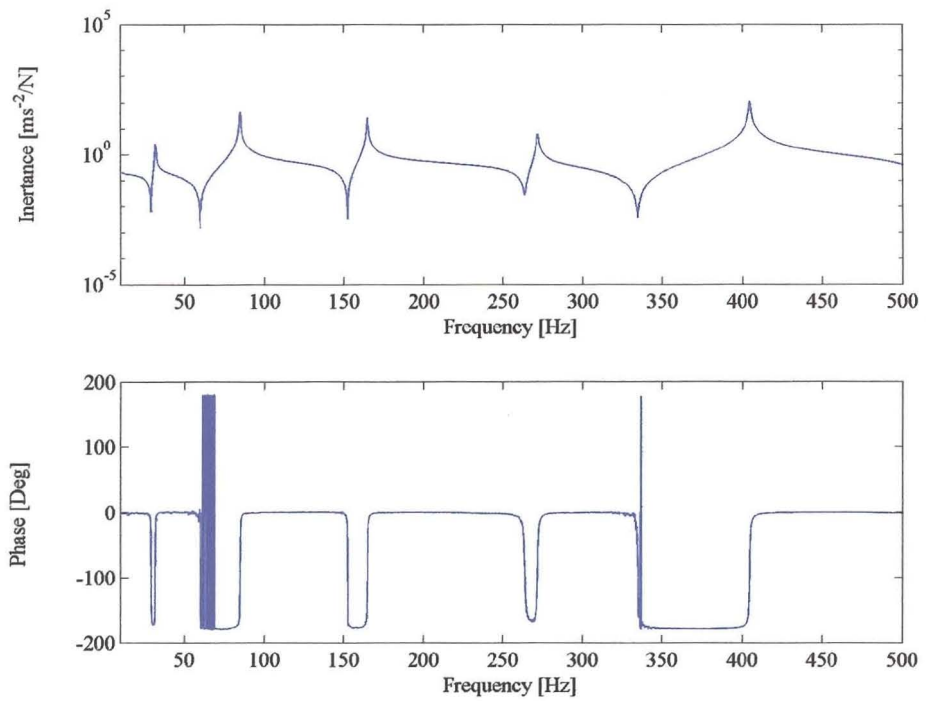

Figure 5.16 – Measured point inertance for the free-free beam corresponding to reference position 8

Figure 5.17 shows the ASD of the actual input forces as measured directly with the force transducers. In the figure, F_a denotes the force measured at position 8, while F_b is the force measured at position 5. Even though the drive signals to the shakers were completely uncorrelated, the measured force signals exhibited some correlation due to the interaction of the excitation system with the structure (Maia *et al.*, 1997). The correlation between the input forces was also evident in the Cross Spectral Densities (CSD) of the input forces, F_{ab}. The correlation components were significant in magnitude so that it was deemed advisable to include their contribution in the force identification process.

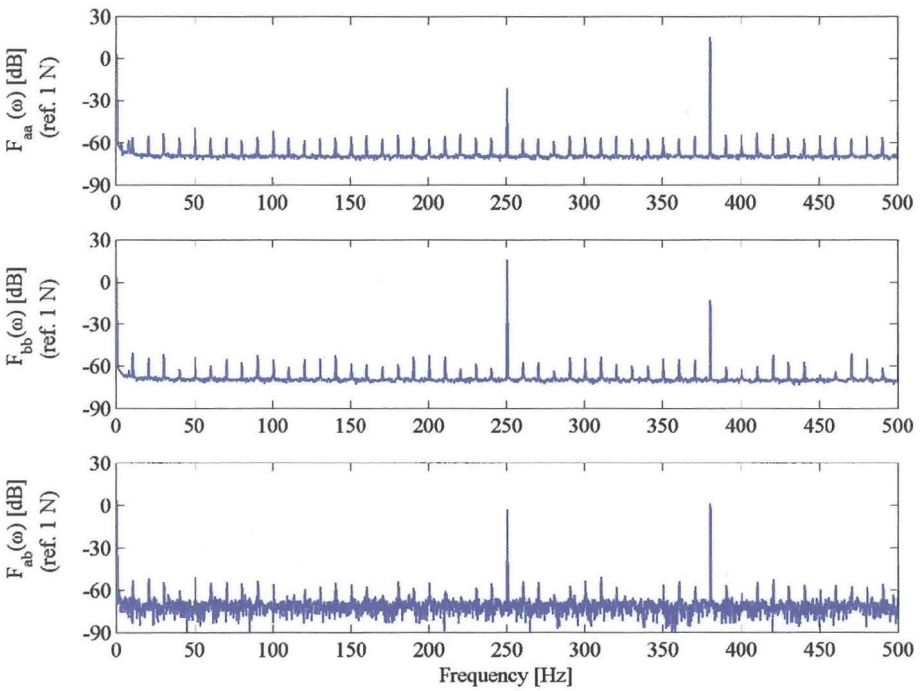

Figure 5.17 – ASD (F_a and F_b) and CSD (F_{ab}) of the two harmonic forces applied to the free-free beam

5.3.3 Force Determination Results

Equation (5.1) can be defined in terms of the spectral density function as:

$$[G_{ff}(\omega)] = [H(\omega)]^{+}[G_{xx}(\omega)][H(\omega)]^{T+} \tag{5.4}$$

For the noise-free case, the rank of the measured acceleration matrix, $[G_{xx}]$, should be equal to the number of linearly independent forces exciting the beam. The rank of the response matrix can be evaluated by applying SVD to the matrix. However, if the forces are not independent, the rank will be less than the number of forces (Elliott *et al.*, 1988).

The measured acceleration matrix was of full rank. This can be attributed to the presence of the measurement noise that spuriously increased the rank of the response matrix. Figure 5.18 shows the singular values of $[G_{xx}]$ and gives no clear indication of the 'true' rank because of the noise contaminating the response.

The full rank matrix $[G_{xx}]$ cannot be substituted into equation (5.4) since the small singular values can falsely dominate the pseudo-inversion and render inaccurate force estimates. Truncating the singular values to reflect the number of independent forces can ameliorate the force estimates. In practice the truncation point of the number of singular values is not always clear, especially when considerable measurement noise is present in the data (Elliott *et al.*, 1988).

The forward problem was solved with the directly measured forces.

$$[G_{xx}(\omega)] = [H(\omega)][G_{ff}(\omega)][H(\omega)]^T \tag{5.5}$$

and the SVD of $[G_{xx}]$ revealed that the rank of the acceleration matrix is indeed one, as depicted in Figure 5.19. The absolute values of the higher-order singular values were of the order 10^{-4} and below and can for all practical purposes be considered as negligible.

Unfortunately, in a real-world application the direct forces will not be available and it may be difficult to determine the 'true' rank of the noise contaminated response matrix.

The $[G_{xx}]$ matrix was recalculated for the truncated singular values and the discrete forces were estimated from equation (5.4). It is apparent from the results in Figure 5.20 that there is some difficulty in predicting the accurate forces at the forcing frequencies. This resulted in an elaborated investigation to find probable causes and explanations for the behaviour noted. The response matrix, as calculated from the forward problem, was substituted into the force identification algorithm and produced excellent force predictions. Next, the accuracy of the inertance matrix and measured accelerations were considered. The individual frequency response functions from the MIMO excitations were compared with previous frequency response functions obtained from single input excitations and found to be satisfactory.

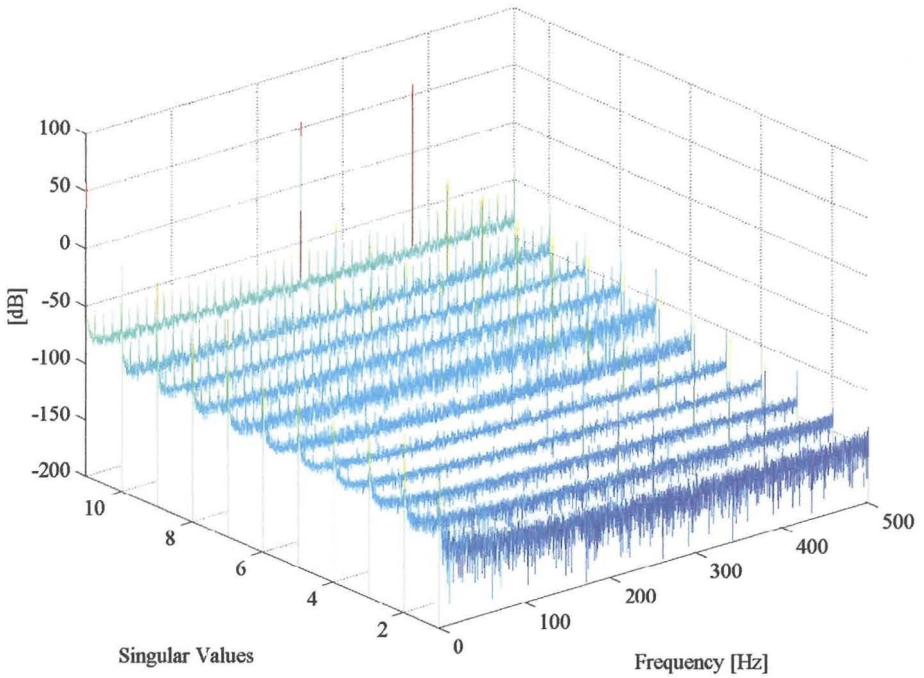

Figure 5.18 - Singular values of the measured response matrix, $[G_{xx}]$

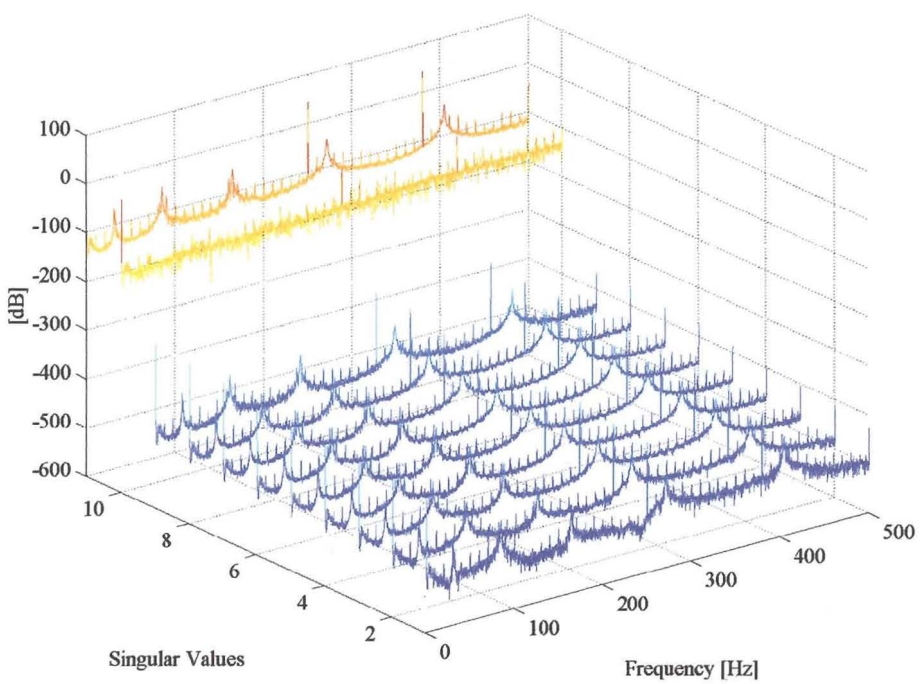

Figure 5.19 - Singular values of the response matrix, $[G_{xx}]$, determined from the forward problem

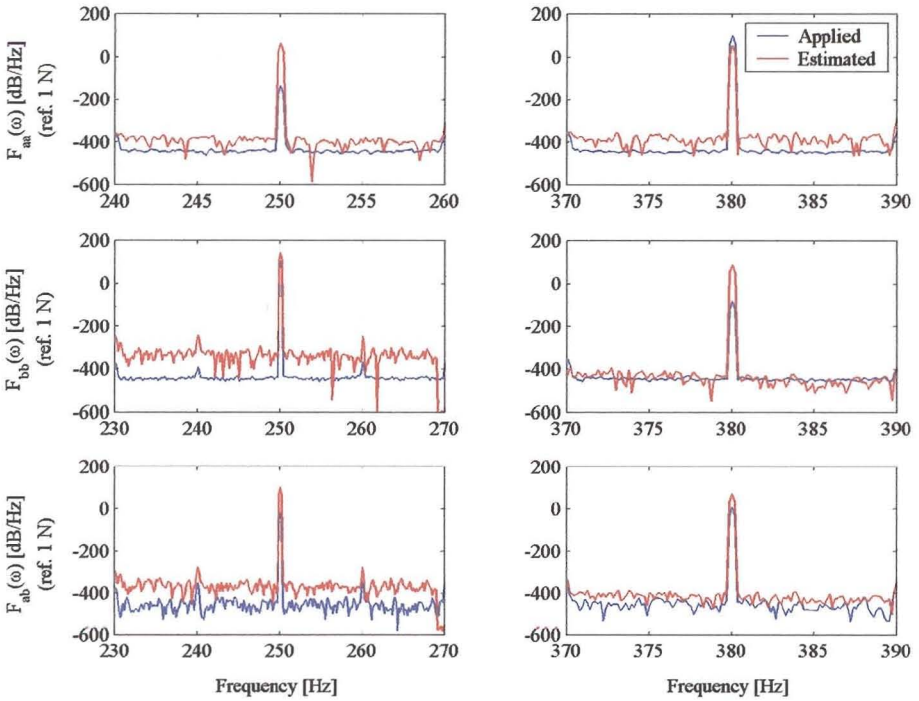

Figure 5.20 – Comparison of measured and estimated forces for the free-free beam

Comparison between the measured accelerations and accelerations computed from equation (5.5) differed significantly (Figure 5.21). Although the presence of considerable noise may contaminate the measured accelerations, the deviation might not be attributed solely to the influence of measurement noise. At first the measured accelerations were thought to consist of the acceleration of the center of mass superimposed on the beam's response subjected to the force inputs. Further investigation revealed this to be an unlikely cause, since the strain measurements strange enough exhibited the same type of behaviour. The only probable explanation was found in a work published by Ojalvo and Zhang (1993: pp. 171):

"Since the ill-conditioning of algebraic equations is dependent upon the zero and near-zero eigenvalues of the coefficient matrix, it is possible to interpret the original equations as those associated with the forced response of a free-free system, or one for which an otherwise structurally stiff system is suspended by very soft springs. In such cases, the zero (or near-zero) eigenvalues represent rigid (or near-rigid) body modes ... small errors in the right hand side may be viewed as static imbalance terms. These would have little effect if the system were restrained (i.e. no zero frequency) but are disastrous for unrestrained systems, and over time can produce large drifts in the system."

The above explanation was taken as the probable cause for the observed behaviour. In addition it was decided to refrain from continuing the force identification on this experimental setup and to progress to the assessment of a restrained system.

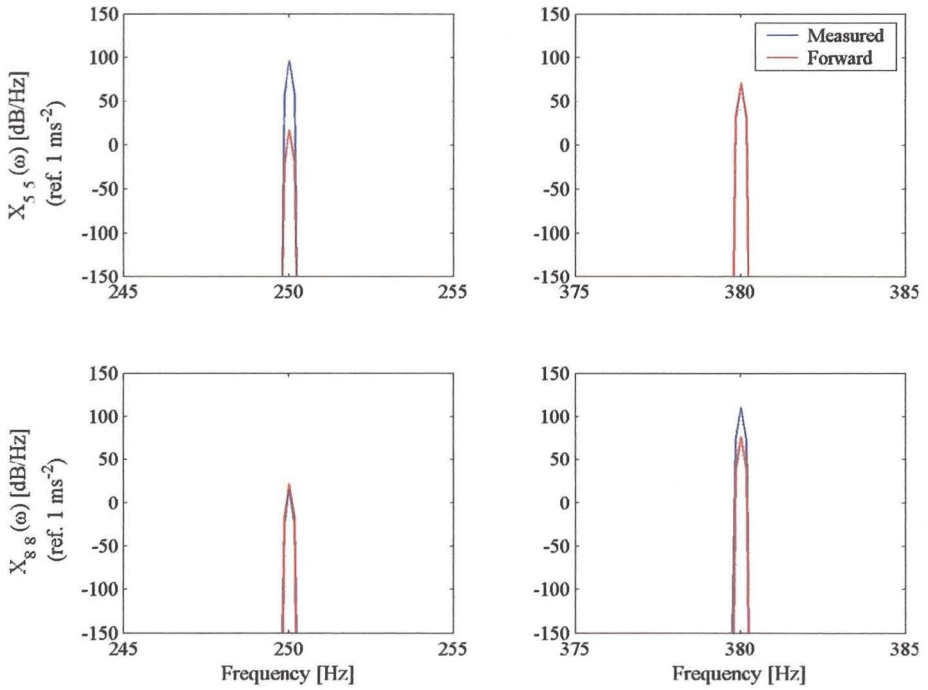

Figure 5.21 – Comparison of the measured and calculated accelerations for the free-free beam

5.4 TWO HARMONIC FORCES: HINGED-HINGED BEAM

This section presents an attempt to apply the force identification process to infer two harmonic forces acting on a hinged-hinged beam. The effect of constraints on both frequency domain methods was investigated.

5.4.1 Details of the Experimental Set-up

The hinged-hinged beam was invoked once again to determine two harmonic forces applied at positions 5 and 8 on the beam.

5.4.2 The Measurements

The measurement procedure described in Section 5.3.2 was repeated, i.e. the inertance frequency response functions were measured first through the use of MIMO excitation. The beam was then subjected to two simultaneous harmonic forces applied at positions 5 and 8 with a frequency content of 380 Hz and 250 Hz, respectively. The point inertance corresponding to reference position 5 is depicted in Figure 5.22, while

the point inertance of reference position 8 in shown in Figure 5.23 (the entire set being represented in Appendix D).

Figure 5.24 shows the ASD of the actual input forces as measured directly with the force transducers. In the figure, F_a denotes the force measured at position 8, while F_b is the force measured at position 5. In contrast to the previous case, the correlation components were orders in magnitude smaller than the actual force components and were considered as negligible. Nine acceleration signals were measured corresponding to position 2 to 10.

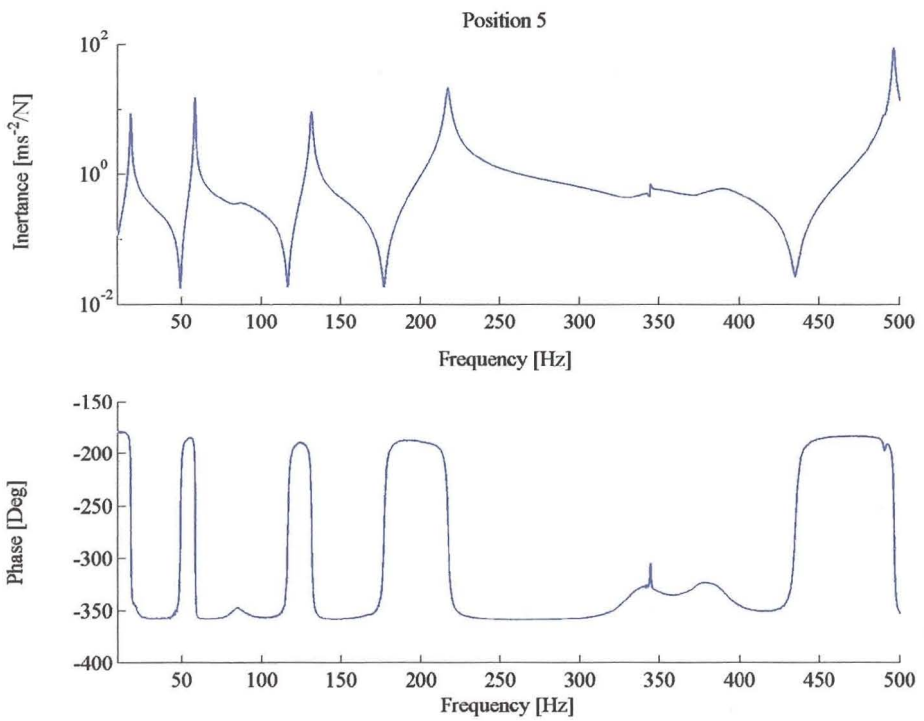

Figure 5.22 – Measured point inertance for the hinged-hinged beam corresponding to reference position 5

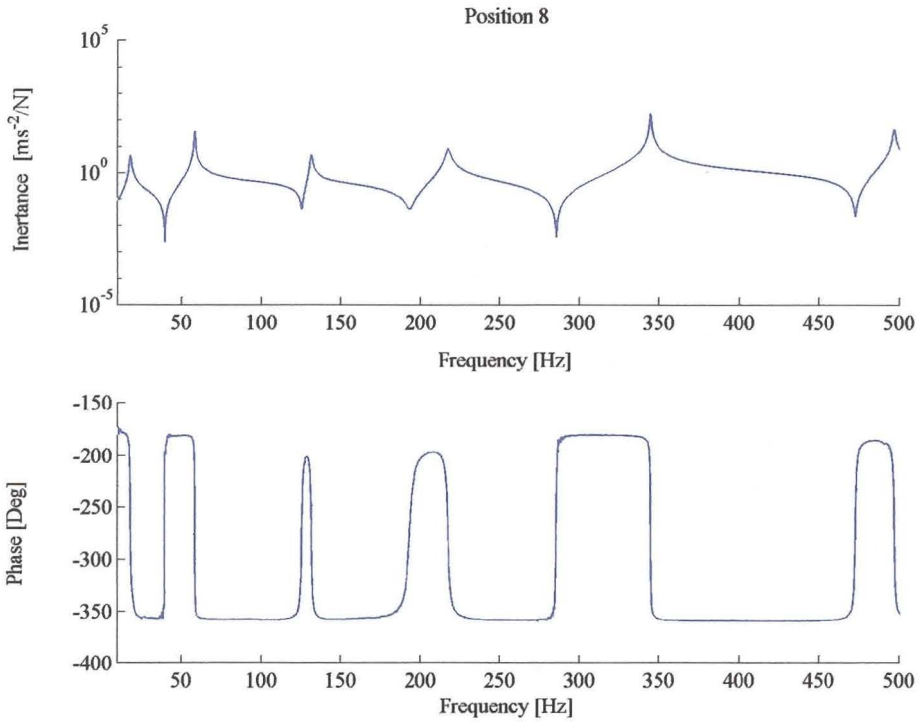

Figure 5.23 – Measured point inertance for the hinged-hinged beam corresponding to reference position 8

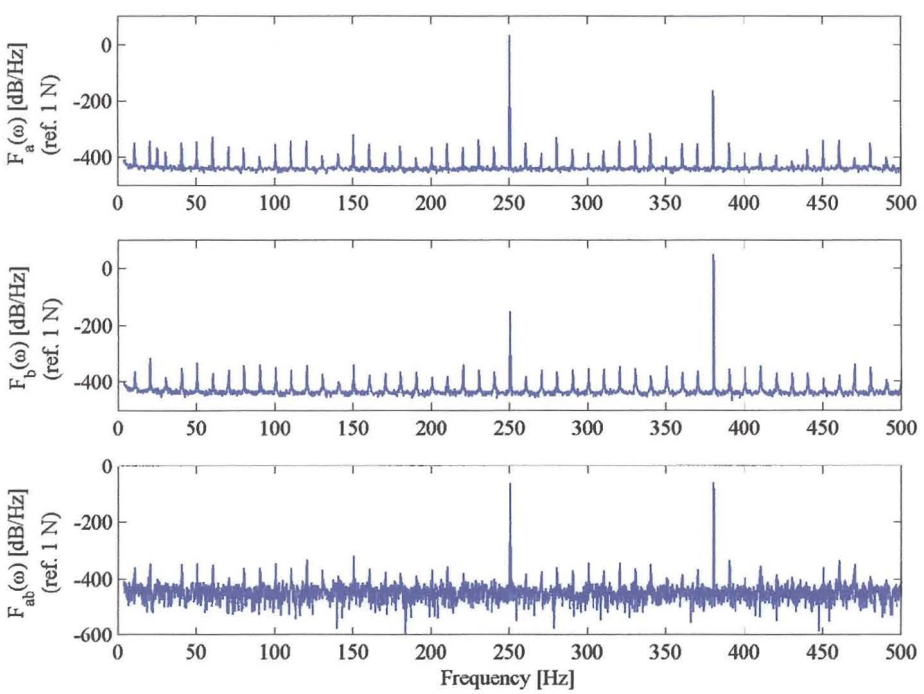

Figure 5.24 – ASD (F_a and F_b) and CSD (F_{ab}) of the two harmonic forces applied to the hinged-hinged beam